CIENCIA 13(2), 250 - 267, 2005
Maracaibo, Venezuela

Study of the activity of Pt-Fe, Pd-Fe and Pt-Cu structured bi-metallic catalysts. Oxidation of VOC: toluene and ethyl acetate

Marcos Rosa-Brussin[1*], Juan Mendialdua[2], Rodrigo Casanova[2], Pedro Hoffmann[2], Alexander Torres[1], Fulgencio Rueda[2], Alfonso Rodriguez[2] y Humberto Rojas[1]

[1]Centro de Catálisis, Petróleo y Petroquímica, Facultad de Ciencias, U.C.V. Apdo. Correos 47102, Caracas 1021, Venezuela. [2]Laboratorio de Física de superficies, Facultad de Ciencias, U.L.A. Mérida.

Recibido: 16-09-04. Aceptado: 15-03-05

Abstract

In this work, Pt-Fe and Fe-Cu bi-metallic catalysts supported on monolithic structures composed of a clay mixture with alumina and zeolite FMI (3% Fe), were prepared separately. The incorporation of the metals was carried out using the simultaneous impregnation method in an approximate time of 30 min. then dried in air and calcinated for 4 h at 500°C. The catalysts obtained were used for VOC oxidation. For all catalysts studied, toluene completely oxidized to CO_2 and H_2O. In the case of ethyl acetate, at relatively low temperatures, partial oxidation products such as ethanol, ethers, acetic acid and acetaldehyde were formed. While oxidation was complete above 280°C. For Pt-Fe catalysts, the influence of the catalytic bed size in the activity was studied. The monolith with the greatest length (6 cm) was the most efficient, reaching toluene conversion > 90%, at elevated flow rate and lower temperatures than those of the remaining catalysts: Pd-Fe and Pt-Cu. The existence of extensive surface zones was determined by the SEM (mapping) technique, where the Pt-Fe and Pd-Fe bi-metallic pair separately, are associated. Iron improves dispersion of Pt microcrystals. XPS results obtained for the Pt-Fe catalyst, indicate an electronic promoter effect between Pt and Fe.

Key words: Monolith; Pd; Pt; VOC; oxidation; XPS; SEM.

Estudio de la actividad de catalizadores bimetálicos estructurados Pt-Fe y Pt-Cu. Oxidación de COV: tolueno y acetato de etilo

Resumen

En el presente trabajo se prepararon separadamente catalizadores bimetálicos soportados sobre estructuras monolíticas Pt-Fe soportados por un material compuesto de una mezcla de arcilla con alúmina y Fe-Cu sobre el material formado por arcilla y una zeolita FMI (3% Fe). Los metales fueron incorporados al monolito por impregnación simultánea, secados en aire y calcinados por 4 h a 500°C. Los catalizadores fueron usados para la oxidación de compuestos orgánicos volátiles (VOC). Con todos los catalizadores utilizados, el tolueno se oxida completamente a CO_2 y H_2O. Al emplear acetato de etilo, a temperaturas relativamente bajas, se forma-

* Autor para la correspondencia. E-mail: mrosabru@strix.ciens.ucv.ve

ron productos de oxidación parcial, tales como etanol, éter, ácido acético y acetaldehído. Por encima de 280°C la oxidación fue completa. Para los catalizadores Pt-Fe se determinó la influencia del tamaño del lecho en la transformación de los hidrocarburos. El monolito de 6 cm fue el más eficiente. Mediante la técnica de microscopía electrónica de barrido (SEM-Mapping) fue posible determinar amplias zonas en la superficie del monolito, donde se superponen los pares metálicos Pt-Fe y Pd-Fe separadamente. Los resultados XPS obtenidos para el catalizador Pt-Fe indican un cambio en el estado electrónico del Pt y del Fe.

Palabras clave: Monolítica; oxidación; Pd; Pt; VOC; XPS; SEM.

1. Introduction

Emissions of volatile organic compounds (VOC) to the atmosphere, contribute to the formation of photochemical smog which causes damage to plants and animals, in addition to eye irritation and respiratory problems in humans. In some people, exposure to VOC can also contribute to an increased risk of developing cancer. On the other hand, some VOC such as chlorofluorocarbons (CFC), contribute to the destruction of the stratospheric ozone layer and others, such as methane, absorb significant quantities of solar energy contributing to the greenhouse effect and, therefore, to global warming. Owing to all this, there is currently a clear tendency towards the reduction of VOC emissions into the atmosphere. Hence, many countries are changing their legislation on VOC emissions and the rest are also studying these changes to evaluate when they may do so as well.

The use of solvents in different industrial processes ranging from the use of paints and varnishes, adhesives, cleaning and degreasing or agricultural produce industries, give rise to a widespread problem depending on the degree of development of the country and with common characteristics, yet at the same time with singularities demanding adapting of solutions to each particular case.

The first steps to be taken to minimize this problem consist in the optimization of the process and the change of the raw material used. However, there are limitations in both available technologies and the costs involved. On the other hand, each country has strategic criteria that condition the most suitable raw materials in each case. All of this results in secondary measures, i.e., post-treatment of emissions to reduce their VOC content, which is currently the fastest tool used in most cases.

In this sense, the most efficacious technologies are thermal or catalytic oxidation and adsorption. Each one of these has advantages and inconveniences, therefore, each concrete case must be analyzed separately in order to select the most suitable. Since thermal oxidation consumes more energy, the current tendency is to use catalytic oxidation and adsorption. Both have one thing in common, which is that the core of the technique, the point determining its efficaciousness and, ultimately, the cost, is the solid employed: catalyst in one case, adsorbent in the other. Availability of this solid with good properties and at competitive prices is the fundamental point to design and apply these technologies. Therefore, the most adequate material must be a balanced between properties and prices and, thus, very related to the raw materials available in each country.

With regard to catalysts, there are two great active phase options: noble metals, mainly Pt and Pd, and transition metals oxides, Mn, Cr, Cu, Ni, etc. (1). In general, the noble metals are more active, expensive and sensitive to poisons. On the other hand, oxides are usually less active but cheaper and more resistant to poisons. The Election of one or other will depend on the characteris-

tics of the emission to be treated. In addition, the active phases require a support that helps to their dispersion and stabilization. The nature and preparation of the support may be varied to adapt to the different active phases and their uses.

In the case of adsorbents, there are many materials such as active carbon, zeolites and clays. In addition to price, the fundamental aspects are their interactions with water vapor and VOCs; both groups may be controlled during preparation and activation, and their resistance to the different regeneration protocols (temperature and atmosphere).

It is fundamental to conform both the catalysts and the adsorbents, since emission treatment processes may require minimum charge losses. Therefore, powders and even pellets are usually inadequate and it is preferable to use ceramic monolith or metallic structures (2).

This work is devoted to study the bifunctional Pt-Fe, Pd-Fe and Pt-Cu supported on monolith catalytic structures. Encouraged by promising preliminary results (3, 4) in an attempt to contribute to understand the nature and the catalytic promoter effect of Pt and Pd in the presence of similar amounts of Fe and Cu on the total oxidation of hydrocarbons.

To achieve this objective, a series of Pt/Fe, Pd/Fe and Pt/Cu samples, incorporated by incipient co-impregnation method were tested during the oxidative transformation of toluene and ethyl-acetate. Furthermore, the catalysts were characterized by XPS and SEM techniques.

2. Experimental

The chemical composition of the materials employed in the preparation of monoliths are presented in Table 1.

Catalyst preparation

a) M and Z3 supports were prepared from natural clay mixtures denominated A with alumina (support M) and MFI zeolite type containing iron which is refered as to Fe-MFI, thus obtaining the Z3 support. The particle size in all cases was <100 mesh. A paste with an adequate amount of water was prepared to obtain plasticity of the material, required to provide a honeycomb structure. The monoliths of 2-6 cm in lengh were dried at 110°C and then calcinated in air at 500°C for 5 h, thus obtaining two types of monoliths. The channels had a square shape.

b) Thereafter, the monoliths were co-impregnated with aqueous solutions of salts from transition metals: H_2PtCl_6, $Fe(NO_3)_3$, $Pd(NO_3)_2.2H_2O$ and $CuSO_4$. All impregnations were accomplished in 30 min. In previous works, this time lapse proved to be adequate (5, 6). The solids were then dried and calcinated in air flow at 500°C for 4 h. Three series of catalytic monoliths were obtained in this manner:

   1^{st} series: Pt-Fe; nominal ratio Pt/Fe (1: 1).

   2^{nd} series: Pd-Fe; nominal ratio Pd/Fe (1: 1).

   3^{rd} series: Pt-Cu; nominal ratio Pt/Cu (1: 1).

The bi-metallic catalysts were synthesized using the simultaneous impregnation method from aqueous solutions of the precursor salts. The monolith was submerged in the respective solution for a pre-established period of 30 min. according to a previous study (3). The solid was then dried at room temperature for 12 h and calcinated in an air flow at 500°C for 4 h.

Characterization techniques

XDR analysis were performed on a Philips Difractometer PW 1050/25, using CuKá radiation.

Table 1
Chemical Composition of the materials employed

	Materials		
	Clay	Alumina	Zeolite Fe-MFI
Chemical composition (wt. %)	SiO_2 : 53.98	SiO_2: 0.2	Fe: 3
	Al_2O_3: 16.96	Al_2O_3: 99.50	
	Fe_2O_3: 7.16	Fe_2O_3: 0.10	
	CaO: ≈1	Na_2O: 0.25	
	MgO: ≈1		
	K_2O: ≈1		
	Na_2O ≈1		
	TiO_2 ≈1.1		
	Cr_2O_3: ≈1		
Minerals	Vermiculite Chlorite Quartz (2%) Muscovite Plagioclase	Bohemite	
S_{BET} (m^2/g)	42		322
$Area_{micro}$ (m^2/g)	20 (in pores 30 Å)		293
V_P (Hg) (cm^3/g)	1.38		

The mass chemical composition of the materials employed for M and Z3 synthesis was determined by Atomic Absorption Spectroscopy. The BET area was determined by N_2 adsorption. Elemental analysis of the wall of a selected M cell containing Pt, Pd and Fe was performed by Scanning Electron Microscopy. A Jeol Instrument equipped with EDX Analyzer was employed show X-Ray map and combination map. The XPS spectra were recorded on a VSW Spectrometer PHI 550, using MgKá (1253 eV) as a radiation source. The vacuum system permits a pressure in the range of 10^{-9} mbar.

The surface acidity was determined by pyridine adsorption using a Kahn micro-scale. The mechanical resistance of the monoliths was determined measuring the rupture pressure.

Catalytic Activity

The catalytic activity was determined in a dynamic continuous flow system with integral type glass reactor, where a piece of cut monolith was introduced according to the diameter of the reactor. The catalysts weights was 1.5 - 4.5 g. The reactor was almost adiabatic. The space above and below the catalytic bed (1.7 – 1.5 g) was filled with CSi to allow regularization in flow and preheating of the reaction gases. Analysis of the reagents and products was performed in an HP, gas chromatograph, model 6890, with double detection: TCD and FID. Two packed columns and one capillary column were used: Porapaq S, 0.5 m; Porapaq, Q 3.5 m, Molecular Sieve 13x-3.0m, phenyl-methyl Siloxane/AI_2O_3/KCI – 30m. In addition, a GC-MS, HP-5973 was employed.

VOC concentrations were 2400 ppm for toluene and 8500 ppm of ethyl acetate.

3. Results and Discussion

3.1. Support and Catalyst Characteristics

Table 2 reports textural characteristics of the monoliths in Honeycomb form (M and Z3) prepared from the mixture of materials.

Figure 1 presents the pyridine desorption thermograms for the M and Z3 supports. This desorbed pyridine is from adsorption of this base on the solid acid sites, therefore the amount desorbed is proportional to the concentration of the acid sites in the solid. In this figure, it is clear that the Z3 material has the highest concentration of acid sites, below 400°C.

Table 3 presents the main characteristics of the prepared catalysts.

3.2. Catalytic Activity

a) Activity in the absence of the metallic phase.

The influence of the monoliths and silicon carbide CSi, employed as a catalytic bed filler in oxidative transformation of toluene and ethyl acetate, was determined. The monoliths were 1.8 cm in length, set up in five channels.

At temperatures above 200°C, conversion of the VOCs evaluated is less than 10%.

b) Catalytic activity of supported metals.

All of the Pt and Pd catalysts, oxidize the VOCs producing CO_2 and H_2O.

c) Influence of the support.

The Pt activity results with respect to M and Z3 supports are summarized in Table 4 and Figures 2 and 3. These reflect the scarce influence of the nature of these supports employed, over Pt and Pd activity.

In a previous work, where a more acid support than those used here in was employed, i.e., three times more acid than M, the importance of this property was shown. Greater oxidative disintegration of the hydrocarbon on the surface of the catalyst containing platinum was observed (5). In another work, it was determined that the same 1:1 Pt/Fe ratio was optimum to accomplish conversion values above 90% (4).

d) Promoter Effect

Regarding the nature of the second metal incorporated (Fe or Cu) to the Pt catalyst, the temperature required to achieve conversions higher than 90% is observed to decrease sensitively when the nominal ratio is 1:1. The same is observed for different supports, M and Z3. For Pd, a similar effect to that noted for the Pt catalysts is observed, i.e., the catalytic activity increases when the Pd-Fe nominal ratio is 1:1.

Table 2
Textural characteristics and mechanical resistance of the monoliths.

Characteristics	Materials		
	Clay (A)	Z3 20% Fe-MFI + 80% A	M 30% Al_2O_3 + 70% A
S_{BET} (m^2/g)	42	80	89
S_{Hg} (in pores 30 Å) (m^2/g)	20	16	25
V_p (Hg) (cm^3/g)	1.38	0.37	0.26
R (Kg/cm^2)		248	180
Diameter of channels (mm)		2	2

S_{Hg}: Surface area determined with mercury. V_P: Volume porous. R: Resistance mechanic.

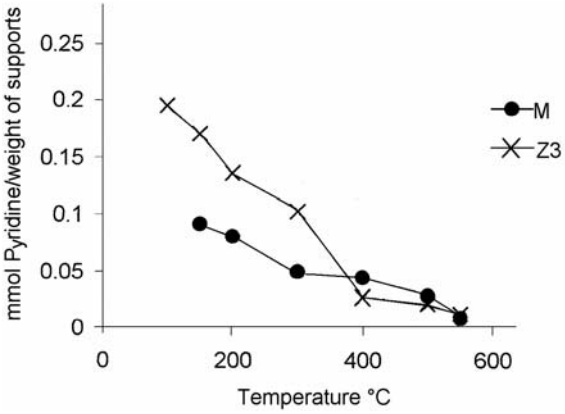

Figure 1. Determination of acidity by means of thermogravimetric analysis of pyridine on M and Z3 supports.

Table 3
Characteristics of the catalysts: M series and Z3 series

Catalyst	Nominal Ratio	Metal Composition (%)	S_{BET} (m^2/g)
Pt/M	-	0.21	77
Pt-Fe/M	1:1	0.24-4.00	77
	1:4	0.13-3.50	98
Pd/M	-	0.16	76
Pd-Fe/M	1:1	0.16-3.50	85
	1:4	0.03-4.44	83
Pt/Z3	-	0.25	77
Pt-Fe/Z3	1:1	0.28-4.10	76
	1:4	0.10-4.12	45
Pt-Cu/Z3	1:1	0.17-0.19	52
	1:2	0.12-0.22	57

The results are summarized in Figures 4 and 5 suggesting a possible electronic promoter effect induced by the presence of a second element impregnated with Pt or Pd on the support. Another plausible explanation, which together with to above, could explain the effect in question, would be more optimum metallic dispersion of the surface Pt and Pd.

For both catalysts, the color microphotographs clearly show this effect, i.e., a different color is assigned separately for each element, red for Fe and green for Pt or Pd. Then, in a separate microphotograph, yellow is assigned to the zones where both elements in the monolith would be associated, thus observing extensive zones of the monolith analyzed with this color, or tinted with yellow and orange, Figures 13 and 14.

e) Contact Time Influence

Table 5 and 6, summarizes the results of activity of diverse catalysts with respect to the Flow rate of toluene and ethyl acetate reactants, respectively.

Generally, both tables present low flow rate, close to 1 L/h, toluene and ethyl acetate transformation is > 90%. This occurs with all catalysts studied, at reaction temperatures ranging between (110-255)°C for toluene (T), and (15-280)°C for ethyl acetate (EA).

At flow rate ≥ than 3 L/h differences of notable activity are observed, depending on the catalyst and particularly on the support used to disperse the active phase. In all cases studied, the Pt/M, Pt-Fe/M series present the highest oxidative activity even at relatively high flow rate.

This study provides a rapid and effective way to select the best active phase with its support, to achieve adequate VOC conversion, depending on the air quality levels required in occupational environments. In addition, it allows for the correct size of the catalyst bed to be manufactured; to achieve this it is sufficient to lengthen the monolith and catalytic converter according to the flow rate established to remove and improve the air to be purified, thus maintaining the adequate level of VOC transformation.

f) Monolith Length Influence

In Figure 6, it is possible to observe that for the Pt-Fe/M catalyst, toluene is more reactive than ethyl acetate. The Pt-Fe/M catalyst of 4 and 6 cm has the same

Table 4
Oxidation temperature with respect to the support

Catalyst	Composition % of metal	S_{BET} (m^2/g)	T (°C) for 90% conversion Toluene	Ethyl Acetate
Pt/M	0.21	77	150	200
Pt/Z3	0.25	77	150	180
Pd/M	0.16	76	150	170
Pd/Z3	0.21	66	180	250

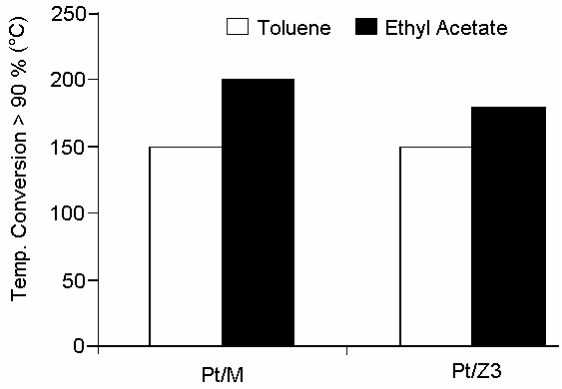

Figure 2. Temperature to convert over 90% of (T) and (AC) as a function of the support.

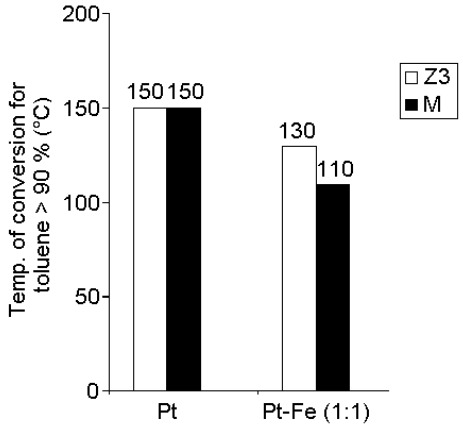

Figure 3. Temperature to convert over 90% of (T) as a function of the support.

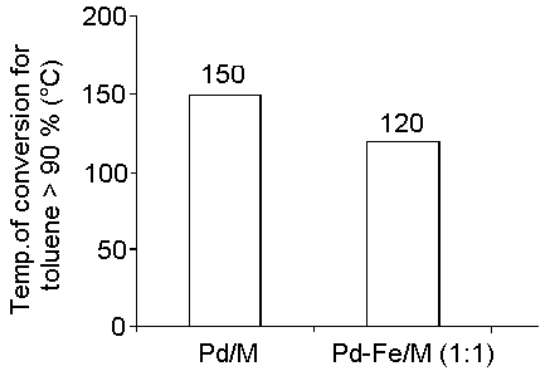

Figure 4. Temperature to convert over 90% of (T) as a function of the Pd-Fe combination.

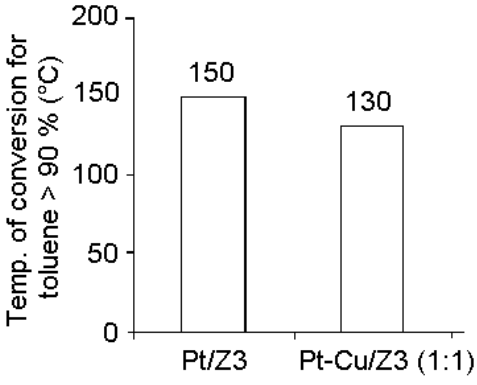

Figure 5. Temperature to convert over 90% of (T) as a function of the Pd-Cu combination.

Table 5
Conversion variation with flow rate (Toluene)

Catalyst	T (°C) > 90%	Flow rate (L/h)			
		1	3	14	25
		Conversión			
Pt/M	150	100	100	91	14
Pt-Fe/M (1: 1) (1: 4)	130	98	92	33	18
	180	99	98	55	22
Pt/Z3	150	97	96	68	-
Pt-Fe/Z3 (1: 1) (1: 4)	110	96	48	12	-
	150	98	82	28	-
Cu/Z3 (1: 1) (1: 2)	200	99	22	2	-
	255	99	88	42	-
Pt-Cu/Z3 (1: 1) (1: 2)	170	99	20	0	-
	170	98	55	9	-

Table 6
Toluene oxidation at different flow rate

Pt-Fe/M Catalyst	Temperature for conversion greater than 90%	Toluene Conversion (%) flow rate L/h			
		1.17	3.14	14	25
2 cm	150°C	96	60	35	-
4 cm	110°C	99	86	74	65
6 cm	110°C	100	100	95	88

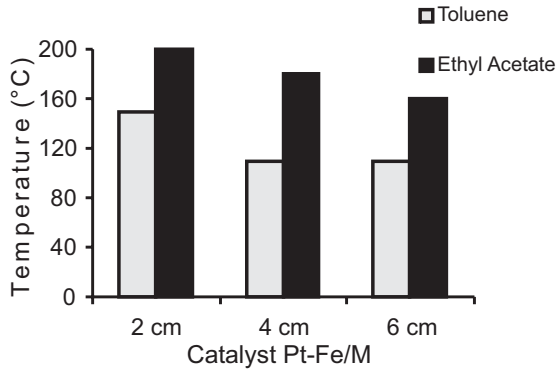

Figure 6. Conversion temperature 90% in toluene and ethyl acetate oxidation with respect to monolith length at 1.17 L/h flow rate.

conversion temperature for toluene (110°C) at a flow rate of 1.17 L/h. It is not reliable to work at temperatures below 110°C owing to the competitive effect of the water with the reactant.

g) Temperature Influence

The influence of the reaction temperature regarding toluene and ethyl acetate conversion to different monolith sizes is represented in Figures 7 and 8.

In Figure 7, the difference in the three catalysts at low temperatures is observed. Especially, in the 2 cm catalyst with respect to the 4 and 6 cm catalysts, until they equalize at an approximate temperature of 130°C.

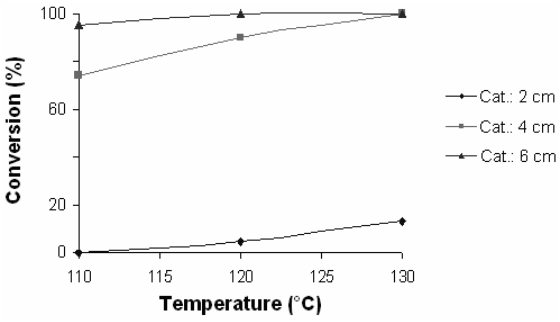

Figure 7. Pt-Fe / M catalyst activity (0.21%) (1:1) regarding reaction temperature Toluene oxidation (2362 ppmv). Flow rate: 14 L / h.

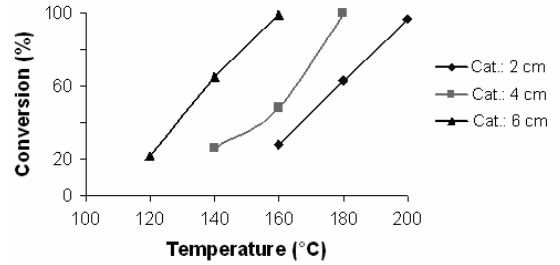

Figure 8. Pt-Fe catalyst activity (1:1) (0.21%) regarding reaction temperature Ethyl acetate oxidation (8464 ppmv). Flow rate: 14 L / h.

Even thought, the 2 cm catalyst activity is much lower with respect to the other two catalysts. In Figure 8, for ethyl acetate a marked difference among the three catalysts is observed and, as expected, the 6 cm catalyst presents the highest activity, followed by the 4 and 2 cm monoliths respectively.

h) Flow rate Influence

Effect produced by flow rate variation maintaining a fixed reaction temperature, is observed.

Figures 9 and 10 present the influence of flow rate over toluene and ethyl acetate conversion respectively. The 6 cm catalytic monolith transforms more efficiently the VOC selected. The activity is maintained abo-

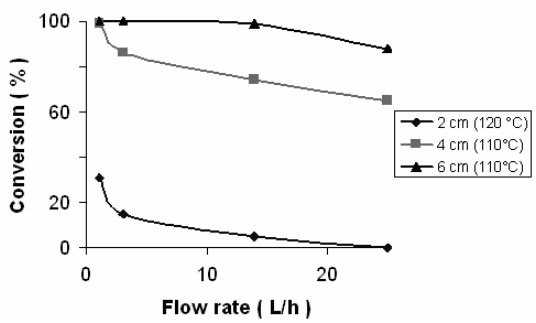

Figure 9. Toluene oxidation (2362 ppmv) at a temperature ranging between 110°C and 120°C using the Pt-Fe / M catalyst (1:1) (0.21%) at different lengths and with respect to flow rate.

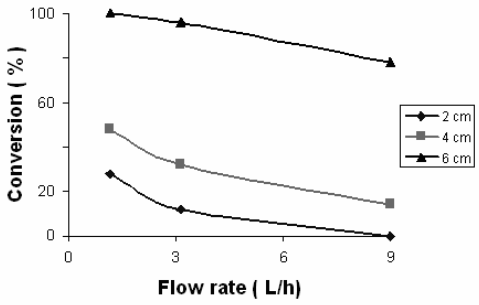

Figure 10. Ethyl acetate oxidation (8464 ppmv) at 160ºC reaction temperature with respect to Pt-Fe / M catalyst length (1:1) (0.21%) and at different flow rates.

ve the 90% conversion, up to flow rate of 25 L/h for toluene and 9 L/h for ethyl acetate, at temperatures ranging from 120 to 160 °C.

Below, the Table 7 present the results obtained in the experiments performed with diverse bed lengths, by varying the flow rate of the reactants.

Table 8 summarizes the conversion obtained in ethyl acetate and toluene simultaneous oxidation at different flow rates using the 6 cm length catalyst.

Table 7
Ethyl acetate oxidation at different flow rate

Pt-Fe/M Catalyst	Conversion temperature (90%)	Ethyl acetate conversion (%) flow rate L/h			
		1.17	3.14	9	14
2 cm	200°C	97	84	-	49
4 cm	180°C	100	84	-	75
6 cm	160°C	100	96	78	-

Table 8
Toluene and ethyl acetate conversion when they react simultaneously using the 6 cm length Pt-Fe / M catalyst

Reagent	Temperature for conversion greater than 90%	Conversion (%) flow rate L/h			
		1.17	3.14	9	14
Toluene	110°C	100	100	97	92
Ethyl Acetate	140°C	100	53	32	-

3.3. Metals on the monolith surface

Scanning Electron Microscopy

Using Scanning Electron Microscopy (SEM) technique, it is possible to obtain information on the supported metal particles, such as their size and dispersion, in addition to the morphology.

Micrographies of the Pt/M and Pt-Fe/M solids are shown in Figures 11 and 12, showing that the presence of iron notably improves the platinum dispersion.

In addition to the above, in Figure 13 and 14 mapping for the Pt-Fe/M and Pd-Fe/M solids was carried out to determine whether or not both co-impregnated metals are superficially associated. For both catalysts, the color microphotographs clearly show this effect: i.e., a different color is assigned for each element separately, red for iron and green for platinum and palladium. Then, in a separate microphotograph, yellow is assigned to the zones in which both elements on the monolith would be associated. In this manner, extensive zones of the monolith surface are observed in that color, or tinted between yellow and orange.

3.4. XPS Characterization of support and Pt catalyst

The materials studied were Pt/M and Pt-Fe/M, where M represents the monolithic support.

The M support was studied after calcination at 500°C in air atmosphere (AA), and after H_2 reduction (26 h at 580°C, 10^{-5} mbar of H_2). The Pt/M and Pt-Fe/M systems in AA conditions, after treatment with O_2 (15 h at 500°C and 10^{-5} mbar) of O_2 are studied below.

Support M.

The main components, apart from the oxygen, and the ratios between the number of atoms, per unit of volume, of the different elements are presented in Table 9.

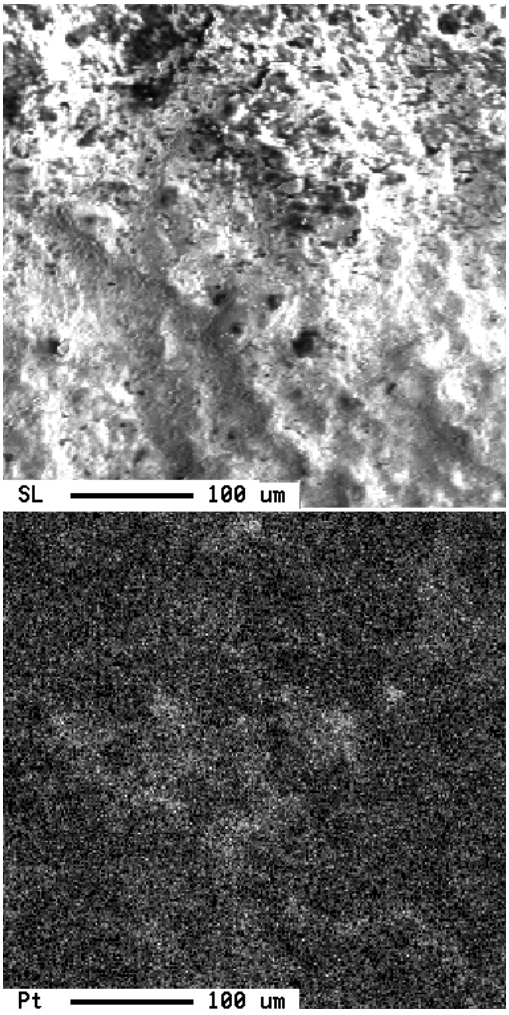

Figure 11. Microphotographs of Pt/M catalyst.

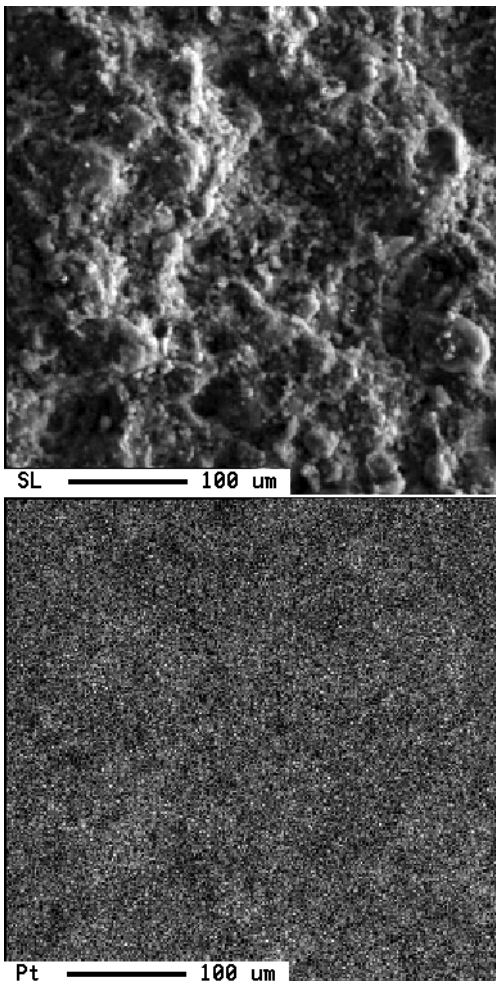

Figure 12. Microphotographs of Pt-Fe/M catalyst.

The above table, demonstrates that the sample contains, approximately:

- 4 atoms of Si for each 5 atoms of Al; 9 atoms of Si for each atom of Fe; 25 atoms of Si for each 4 atoms of Mg; 16 atoms of Si for each atom of Na; 1 atom of Na for each 2 atoms of Fe; 3 atoms of Mg for each 2 atoms of Fe as summarized in the following inequalities:
  Al> Si> Mg> Fe> Na

The amount of oxygen present is higher than That it should be if those elements were under the form of the SiO_2, Al_2O_3, Fe_2O_3, MgO and Na_2O oxides. This may be due to the possible content of structural H_2O in the clay.

- Treatment with H_2 has the following repercussions on the surface:
- the ratio N_{Si}/N_{Al} is practically maintained.
- the Fe amount decreases compared to that of Al.
- the Mg amount increases greatly compared to that of Fe (i.e., there is a migration to the surface).
- the Mg amount strongly increases compared to that of Si.

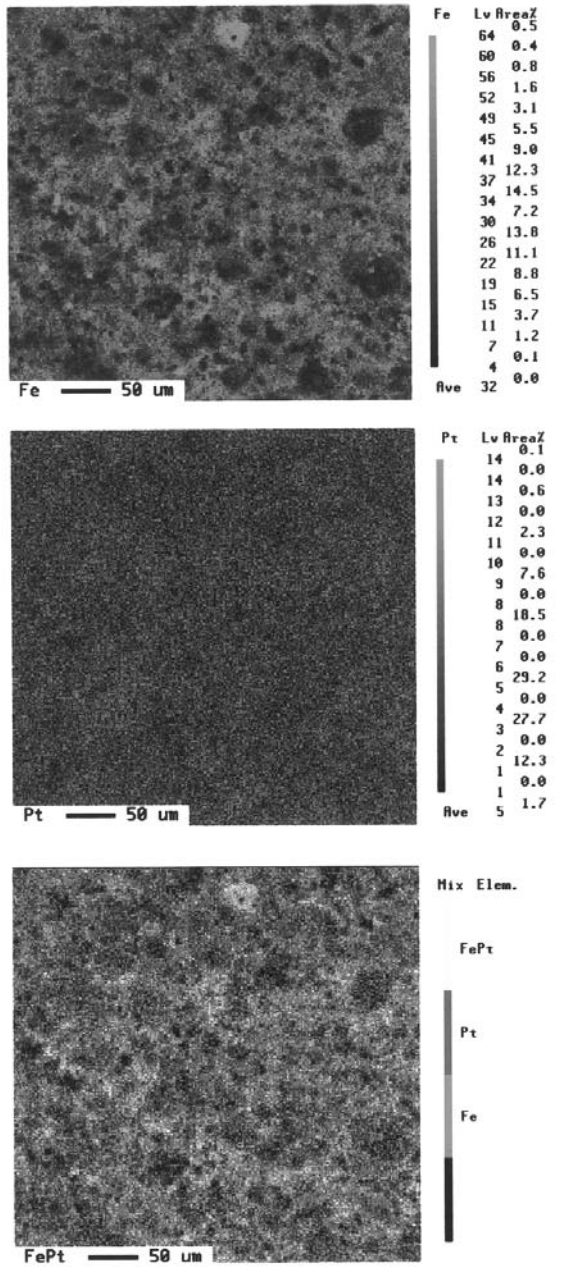

Figura 13. Microphotographs of Pt-Fe/M. Mapping of Pt, Fe and Pt-Fe.

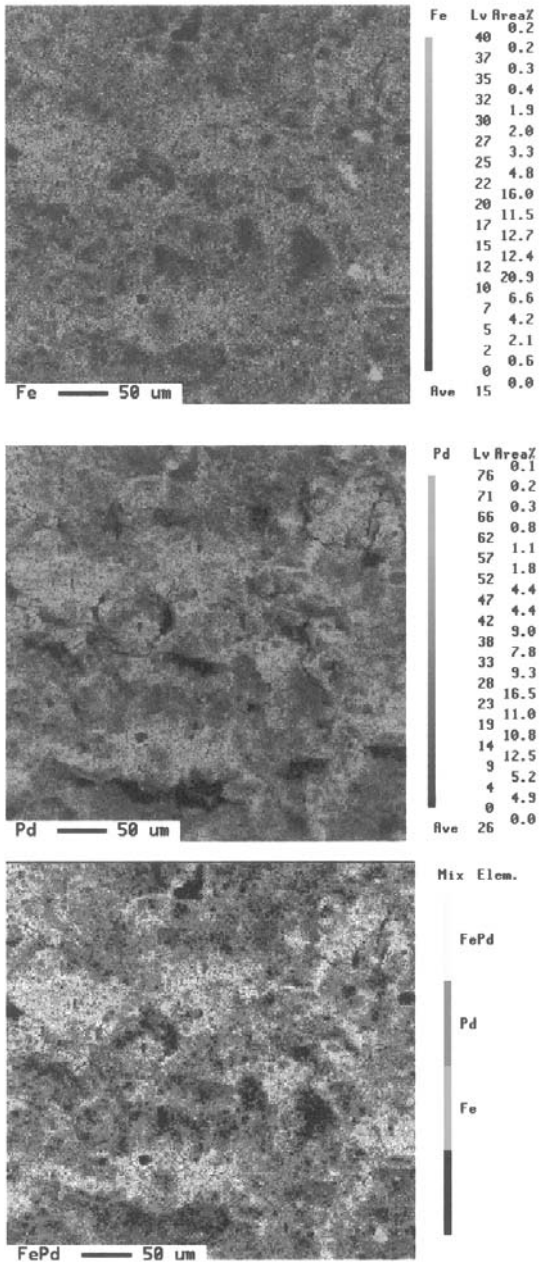

Figura 14. Microphotographs of Pt-Fe/M. Mapping of Pt, Fe and Pt-Fe.

- the Na amount strongly decreases compared to that of Fe.
- an oxygen excess continues to exist.

With regard to the binding energies, Table 10 shows the differences of energy among the O_{1s}, and Al_{2s}, and Si_{2s} level, as well as between $Fe_{2p3/2}$ and O_{1s}.

Table 9
Main elements in M and their ratios

Sample	N_{Si}/N_{Al}	N_{Si}/N_{Fe}	N_{Al}/N_{Fe}	N_{Si}/N_{Mg}	N_{Si}/N_{Na}	N_{Mg}/N_{Fe}	N_{Na}/N_{Fe}
M (AA)	0.85	9.03	10.63	6.26	16.00	1.44	0.56
M (H_2)	0.80	9.23	11.54	5.16	21.53	1.79	0.43

Table 10
Differences of energy (eV)

Sample	O_{1s}-Al_{2s}	O_{1s}-Si_{2s}	O_{1s}-Al_{2p}	Fe_{2p}-O_{1s}
M (AA)	412.4	378.0	457.2	181.6
M(H_2)	412.2	377.8	457.1	182.5

After examining these, it may be concluded that neither the Si nor the Al undergo notable modifications with treatment in H_2 and the variation observed in Fe (the difference increases from 181.6 to 182.5 eV) is in the opposite direction to what is expected if this element undergoes a reduction as a consequence of the treatment. On the other hand, the comparison of the spectral region Fe_{2p} in both states show that the peak $2p_{3/2}$ width is the same in both. Changes are observed in the satellite structures of the shake-up type, which involve the unoccupied valence levels, such changes indicating some modification in the Fe chemical environment, Figures 15 and 16.

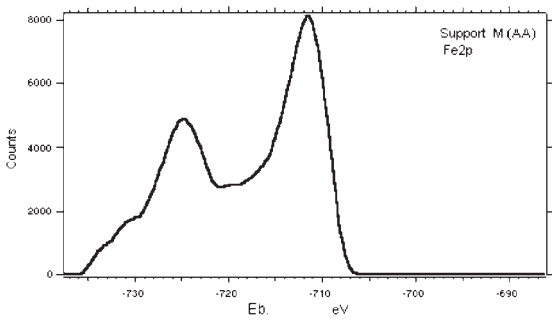

Figura 15. Spectra of the M (AA) sample.

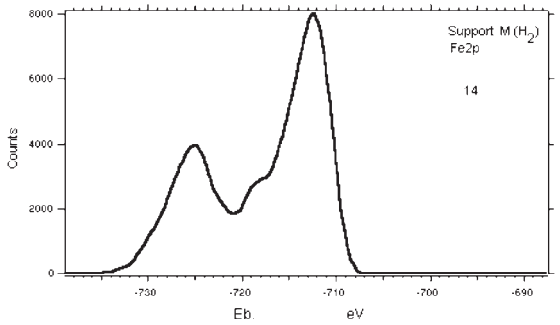

Figure 16. Spectra of the M (H_2) sample.

Pt/M

The results of the quantitative analysis are presented in Table 11.

These may be summarized as follows:

In this sample, in the (AA) state, there are approximately

- 5 Si atoms for every 4 Al atoms; 11 Si atoms for every 1 Fe atom; 17 Al atoms for every 2 Fe atoms; 21 Fe atoms for every 2 Pt atoms; 113 Si atoms for every 1 Pt atom; 89 Al atoms for every 1 Pt atom; 3 Si atoms for every 2 Mg atoms; 7 Mg atoms for every 1 Fe atom

The oxidation treatment (20 h in O_2 at 500°C) results in the following:

- The Si amount decreases slightly compared to that of Al.

Table 11
Quantitative analysis of the Pt/M catalyst

Sample	N_{Si}/N_{Al}	N_{Si}/N_{Fe}	N_{Al}/N_{Fe}	N_{Fe}/N_{Pt}	N_{Si}/N_{Pt}	N_{Al}/N_{Pt}	N_{Si}/N_{Mg}	N_{Mg}/N_{Fe}
Pt/M (AA)	1.27	10.76	8.47	10.52	113.21	89.10	1.52	7.08
Pt/M (O_2)	0.91	10.97	12.05	7.56	82.88	91.10	1.39	7.89

- The N_{Si}/N_{Fe} ratio is maintained.
- The Al amount increases compared to that of Fe.
- The Pt amount increases with that of Si and Fe, and to a lesser measure with that of Al.
- The Si amount decreases slightly compared to that of Mg.
- The Mg amount increases slightly compared to that of Fe.
- When comparing Pt/M in the (AA) state to the M support in the same state, it can be affirmed that in Pt/M
- More Si is seen than Al; More Si is seen than Fe; Less Al is seen than Fe; Less Si is seen than Mg; More Mg is seen than Fe.

Changes are observed in the satellite structures of the shake-up type, such changes indicating some modification in the Pt chemical environment, Figure 17 and 18.

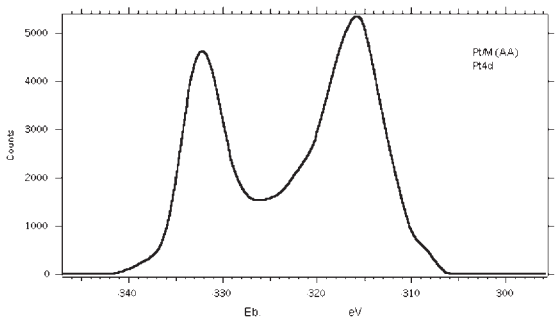

Figura 17. Spectra of the Pt/M (AA) sample.

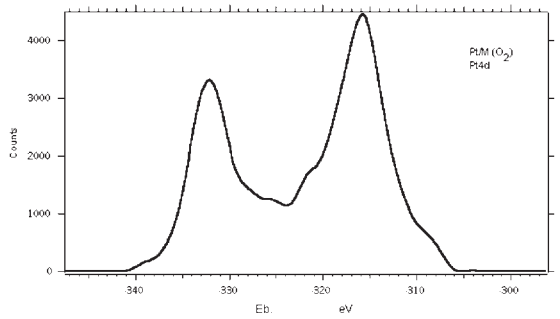

Figure 18. Spectra of Pt/M (O_2) sample.

Pt-Fe/M

The Figure 19 and 20 show the spectra of Pt-Fe/M samples in different environments.

Table 12, reflects the ratios between the number of atoms per unit of volume in the surface region, as summarized approximately as follows:

- 11 Si atoms for every 16 Al atoms; 13 Si atoms for every 7 Fe atoms; 9 Si atoms for every 4 Mg atoms; 4 Mg atoms for every 5 Fe atoms; 17 Fe atoms for every Pt atom; 31 Si atoms for every Pt atom; 45 Al atoms for every Pt atom.

In addition to the elements presented in Table 12, the sample contains a slightly less amount of oxygen than it should do, if these elements were under the form of oxides in their highest degree of oxidation.

Treatment with oxygen has the following repercussions on the surface:

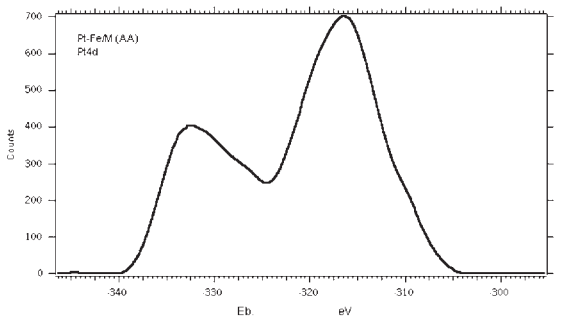

Figure 19. Spectra of the Pt-Fe/M (AA) monolith.

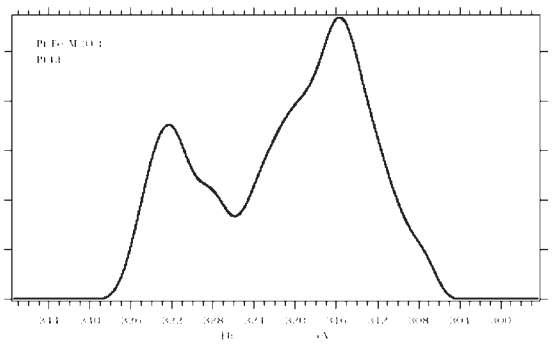

Figure 20. Spectra of the Pt-Fe/M (O_2) sample.

– the Si amount increases compared to that of Al; the Si amount increases compared to that of Fe; the NAl/N_{Fe} ratio is maintained; the Pt amount increases compared to that of Fe, Al and Si; the N_{Si}/N_{Mg} ratio is maintained; the Mg amount increases compared to that of Fe.

Treatment with H_2 has the following effects:

– the N_{Si}/N_{Al} ratio achieved in oxidation is maintained; the Si amount increases compared to that of Fe; it follows the oxidation tendency; the Al amount increases compared to that of Fe; the Pt amount decreases slightly compared to that of Fe, contrary to what occurs in oxidation; the Pt amount decreases markedly compared to that of Si, contrary to what occurs in the oxidation; the Pt amount decreases significatly compared to Al, contrary to what occurs in the oxidation; the Si amount increases compared to that of Mg; the N_{Mg}/N_{Fe} ratio achieved in the oxidation is maintained.

Therefore, it may be affirmed that treatment with H_2 causes the Pt migration outside the surface and in less proportion the Fe.

Comparing this sample to the M support, it is possible to affirm:

– Greater preference of Pt to cover Si than for Al.

– Greater preference of Fe to cover Si than for Al (since the small amount of Pt present would not explain the change of the N_{Si}/N_{Al} ratio between this sample and the M support).

– No preference of Pt and Fe to cover Mg.

The atomic ratio obtained between the Pt and Fe corresponds approximately to a ratio of 1 to 4 in weight.

With regard to the binding energies, Table 13 shows that neither Si nor Al, nor Fe undergo appreciable modifications; however, comparison of the Fe_{2p} region after oxidation and reduction treatment, show that the width of the $2p_{3/2}$ peak, after treatment with H_2, is notably larger than after treatment with O_2, this indicating a certain degree of Fe reduction.

A comparison of both samples in the AA state shows the following results:

– In the Pt/M sample, compared to Pt-Fe/M.

– More Si is seen than Al.

– More Si is seen than Fe.

– More Al is seen than Fe.

– Less Fe than Pt.

– More Si is seen than Pt.

Table 12
Atomic ratios of Pt-Fe / M catalyst in different environments

Sample	N_{Si}/N_{Al}	N_{Si}/N_{Fe}	N_{Al}/N_{Fe}	N_{Fe}/N_{Pt}	N_{Si}/N_{Pt}	N_{Al}/N_{Pt}	N_{Si}/N_{Mg}	N_{Mg}/N_{Fe}
Pt-Fe/M (AA)	0.59	1.61	2.72	22.8	36.7	62.02	2.19	0.73
Pt-Fe/M (O_2)	0.68	1.86	2.73	16.74	31.14	45.70	2.23	0.83
Pt-Fe/M (H_2)	0.69	2.10	3.05	17.92	37.63	54.66	2.50	0.84

Table 13
Energy differences (eV) among the O_{1S}, and Al_{2S}, and Si_{2S} level as well as between $Fe_{2p3/2}$ and O_{1S}

Sample	O_{1S}-Al_{2S}	O_{1S}-Si_{2S}	O_{1S}-Al_{2p}	Fe_{2p}-O_{1S}
Pt-Fe/M (AA)	412.6	378.2	457.3	181.3
Pt-Fe/M (O_2)	412.5	378.2	457.3	181.5
Pt-Fe/M (H_2)	412.6	378.2	457.3	181.4

- More Al than Pt.
- More Mg is seen than Fe.
- Less Si is seen than Mg.

These results may be explained under the hypothesis that, in the Pt-Fe/M sample, with preference Fe covers Si and Al, and the fact that in Pt/M there is less Fe.

When comparing the spectra corresponding to the Fe_{2p} regions in the Pt/M sample with those of the Pt-Fe/M, it may be affirmed that differences exist, both in the AA state and in the oxidation state. These are observed in the shake-up structures present in the region between the $2p_{1/2}$ and $2p_{3/2}$ peaks. In the Pt-Fe/M sample, the presence of two types of Fe is very probable, one pertaining to the M substrate, probably under the form of aluminum-silicate, and another deposited on the surface together with the Pt, probably under the form of some oxide and/or Fe hydroxide.

In observing the spectra corresponding to Pt_{4d} in the Pt/M and Pt-Fe/M sample, enables us to note the presence of two types of Pt in the latter, one related to the Fe of the substrate and another related to the Fe deposited on the surface. The values obtained for the binding energy of the $Pt_{4d3/2}$ level (315.5 eV) in the Pt/M and Pt-Fe/M sample, do not correspond to Pt in metal form.

The differences observed between Fe in the M substrate and in the Pt/M sample, and in the Pd/M sample, could point in the direction of an interaction among this type of Fe and Pt and Pd, since the largest differences arise in the shake-up structure interpeaks, and, as well known, the shake-ups are phenomena involving the valence levels.

Table 14 indicates the values of binding energies of the samples studied.

Conclusions

The presence of iron or copper co-impregnated with Pt or Pd exert an electronic or textural type promoter effect. Metal dispersion of the main active phase seems to be increased.

Table 14
Binding energies, (eV) of peak different of the samples

Sample	O_{1S}	Al_{2p}	Si_{2p}	Fe_{2p}	Auger Ox.	Al_{2s}	Si_{2s}	Pd_{3d}	Pt_{4d}	Mg_{1s}	Na_{1s}
M (AA)	532.0 529.9	74.8	103.0	724.9 711.5	471.4 486.7 507.4	119.6	154.0			1303.4	1072.3
M (H_2)	532.1 529.9	75.0	103.4	725.2 712.4	472.2 486.6 507.3	119.9	154.3			1304.4	1073.4
Pt/M (AA)	532.3 530.1	75.1		726.0 712.6	471.8 485.9 506.9	119.6	154.2		332.1 315.7	1303.8	1073.2
Pt/M (O_2)	532.6 530.4			726.0 712.8	470.4 485.7 506.7	120.1	154.5		331.8 315.4	1304.9	1073.2
Pt-Fe/M (AA)	531.9 530.3	74.6		724.8 711.6	470.8 486.1 506.5	119.3	153.7		332.2 316	1304.1	
Pt/M (O_2)	532.1 530.7	74.8		725.4 712.2	470.8 486.6 507.1	119.6	153.9		332.0 317	1304.5	1073.2
Pt-Fe/M (H_2)	532.2 530.6	74.9		724.8 712.0	472.3 486.4	119.6	154.0		315.7 332.5	1304.7	
Pd/M (AA)	532.4 529.9	75.3	103.3	725.4 713.4	471.4 486.1 507.1	120.1	154.3	340.7 335.4		1304.3	1073.3
Pd/M (H_2)	532.5 529.9	75.4	103.5	724.9 712.3	471.6 486.0 507.0	120.1	154.5	341.0 335.7		1304.4	1073.7

Using the X-ray map (SEM) results, it is possible to determine the existence of extensive superficial zones where Pt and Fe are associated.

The XPS results show an electronic promoter effect between the Pt and Fe, which translates into alterations in the shake-up structure interpeaks, a phenomenon involving the valence levels.

Monoliths of 6 cm in length with 0.21% Pt composition and Pt nominal ratio: Fe close to 1:1, oxidize the selected hydrocarbons to CO_2 and H_2O above 90% conversion; i.e., at 110°C and 160°C for toluene and ethyl acetate, respectively.

For flow rate over 1.7 L/h, it is necessary to increase the temperature somewhat to maintain the >90% conversion level.

For toluene: 110°C up to 25 L/h

For ethyl acetate: 160°C up to 3.14 L/h.

The experimental data obtained must permit construction of a catalytic converter prototype for air purification in working environments.

Acknowledgements

This work was supported by FONACIT-CONIPET project N° 97003734.

References

1. ERTL G., KNÖZINGER H., WEITKAMP J. "Handbook of Heterogeneous Catalysis", Eds Wiley-VCH, Weinheim (Fed. Rep. Germany) Vol. 4, 1997.
2. CYBULSKI A., MOULIJN J.A. "Structured Catalysts and Reactors", Eds. M. Dekker, New York (USA), p. 35, 1998.
3. ROSA-BRUSSIN M., CORREDOR J., CASTRO I., ROJAS H., Torres A. Proceeding XVII Simp. ***Ibero-Am Catalysis***, pp. 1-6, 2000.
4. ROSA-BRUSSIN M., PEÑA J., ROSA-BRUSSIN C., CASTRO I., ROJAS H., TORRES A. Proceedings XVIII Simp. Ibero-Am Catálisis. pp. 1-6, 2002.
5. ROSA-BRUSSIN M., CASTRO SALAZAR I., TORRES A., OSTOS A., ROJAS H., Ng Lee Y. ***Rev Facultad Ing*** UCV 19(1): 107-117, 2004.
6. DE LUCA J.P., CAMPBELL L.E. "Advanced Materials in Catalysis", Materials Science Series, Academic Press, Ed. J. J. Burton, R. L. Garten, New York (USA), pp. 309, 293-324, 1977.